Abo-Sreeaa *et al.*
Journal of Engineering and Applied Science (2023) 70:76
https://doi.org/10.1186/s44147-023-00246-0

Journal of Engineering and Applied Science

RESEARCH Open Access

The impact of blockage on the performance of canal coverage structures

Doaa A. Abo-Sreeaa[1*], Nahla M. AboulAtta[1] and Doaa A. El-Molla[1]

*Correspondence:
doaa.ahmed2912@gmail.com

[1] Irrigation and Hydraulics Department, Faculty of Engineering, Ain-Shams University, Cairo, Egypt

Abstract

Despite the benefits of canal coverage structures, they may turn out to be a significant reason of decreasing canals conveyance efficiency if they are subject to blockage. The difficulty of removing wastes from closed canals further exaggerates the problem. This study investigates the effects of blockage in canal coverage structures, focusing on various cross-sectional shapes and blockage ratios. Seven coverage cross-section shapes, namely the square box, pipe, pipe arch, ellipse, arch, conspan arch, and rectangular box, were studied in combination with 10 different Froude numbers and 10 different blockage ratios. An experimental setup was used in the study along with the HEC-RAS 1D numerical model, which was evaluated through a series of comparative tests.

The study demonstrated that blockage in a canal coverage structure and its extent significantly impairs the structure's hydraulic performance, leading to an increased head loss ratio and a reduced velocity ratio. The extent of this reduction varied with different coverage shapes, and the sensitivity to blockage was found to be the highest in the square box section, followed by the pipe section at the same design Froude number.

A crucial threshold was identified at a blockage ratio of 30% where the performance of coverage structures started to decline sharply, indicating a key maintenance point. Among the shapes studied, the pipe arch had the best performance in terms of head loss reduction, while a rectangular box with a height to width ratio of 2:3 was found to be a close second. Considering the construction complexities associated with the pipe arch, the rectangular box is recommended as the most practical and efficient option for canal coverage structure design. The findings from this study provide valuable insights for engineers and decision-makers involved in canal management and infrastructure planning.

Keywords: Blockage, Canal coverage structures, Culvert, Experimental model, HEC-RAS, Hydraulic structures, Maintenance threshold, Numerical modelling

Introduction

The efficient operation of irrigation systems is critical to sustaining agricultural productivity, particularly in the face of the current water scarcity and increasing population pressures. Central to these systems are the canals that serve as primary conduits for water conveyance, their performance is significantly influenced by their accompanying infrastructure, including weirs, culverts, and bridges [1, 2]. Irrigation canals' function

can be compromised when they pass through residential areas, with the inappropriate disposal of waste leading to decreased efficiency and water quality [3, 4]. In addition to human factors, climate changes and global warming contribute to water losses from irrigation canals due to seepage and evaporation [5–7]. The solution lies in canal coverage structures, which are culvert-like constructions that reduce streambed recharge and evaporation losses [8–10]. In this study, the phrase "canal coverage structure" is employed to encompass a wider array of constructions, extending beyond culverts to include diverse structural designs utilized to cover canals (Fig. 1). However, while a coverage structure is effective in quantity preservation, there are concerns about its impact on water quality. El Baradei and Alsadeq [11] suggest that the covered area should not exceed 32.8% of the total canal surface to maintain optimal DO and BOD levels.

One challenge with canal coverage structures is that they are vulnerable to blockage, a problem amplified by difficult waste removal in closed canals compared to open ones [13, 14]. This blockage, often resulting from the accumulation of waste and sediment (Fig. 2), can significantly reduce the conveyance efficiency of the canals [15, 16]. In fact, the degree of blockage, or blockage ratio, can exert a significant influence on the open channel's water surface profile [17].

Understanding the impact of blockage, researchers have explored how various factors affect the risk and repercussions of this issue. Rigby et al. [16] found that smaller culverts (with an opening less than six meters measured diagonally) are more susceptible to blockage, independent of other variables such as material type or land use. Studies also highlighted the risk of embankment overtopping and failure due to culvert blockage [18].

Other research has investigated the effects of blockage on flood behaviour [19], culvert scour depth [20], and turbulent flow conditions [21]. In relation to canal coverage

Fig. 1 A canal coverage structure passing through a residential area [12]

Fig. 2 Municipal waste accumulation at the entrance of a coverage structure [12]

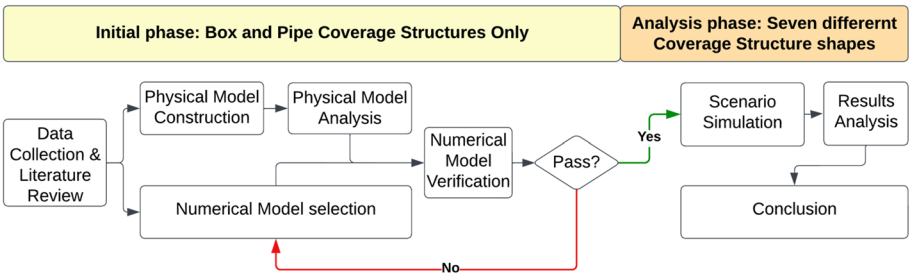

Fig. 3 Flowchart depicting the sequential research methodology, including data collection, model development, verification, scenario simulation, and data analysis stages, with key decision points

structures, studies have examined the effects of different blockage ratios [22] and blockage at the inlet of coverage structures [23, 24].

While substantial work has been done in this field, gaps still persist. The effects of inlet blockage on open channel performance still require more investigation. Moreover, most studies have focused on pipe and box-shaped structures [25, 26], leaving other shapes less explored. Addressing these gaps, this study aims to evaluate the effects of blockage at the inlet of variously shaped canal coverage structures on their hydraulic parameters. The investigation, conducted via experimental and numerical modelling, measures the changes in water levels and velocities due to blockage. The main objective of the study is to contribute to the field's understanding of how to best design and manage canal coverage structures to reach an optimum performance.

Methods

Research methodology

The research methodology consisted of several stages to understand the impact of canal coverage structures and their blockage on the hydraulic performance of canals (Fig. 3). The study initiated with data collection and a review of the existing literature to identify the research gaps. Next, a physical model was developed to represent canal coverage structures. This stage, represented in Fig. 4, established a baseline to verify the validity of the numerical model.

The HEC-RAS 1D numerical model was the chosen tool for conducting numerical modelling in this research. This selection was based on recommendations provided

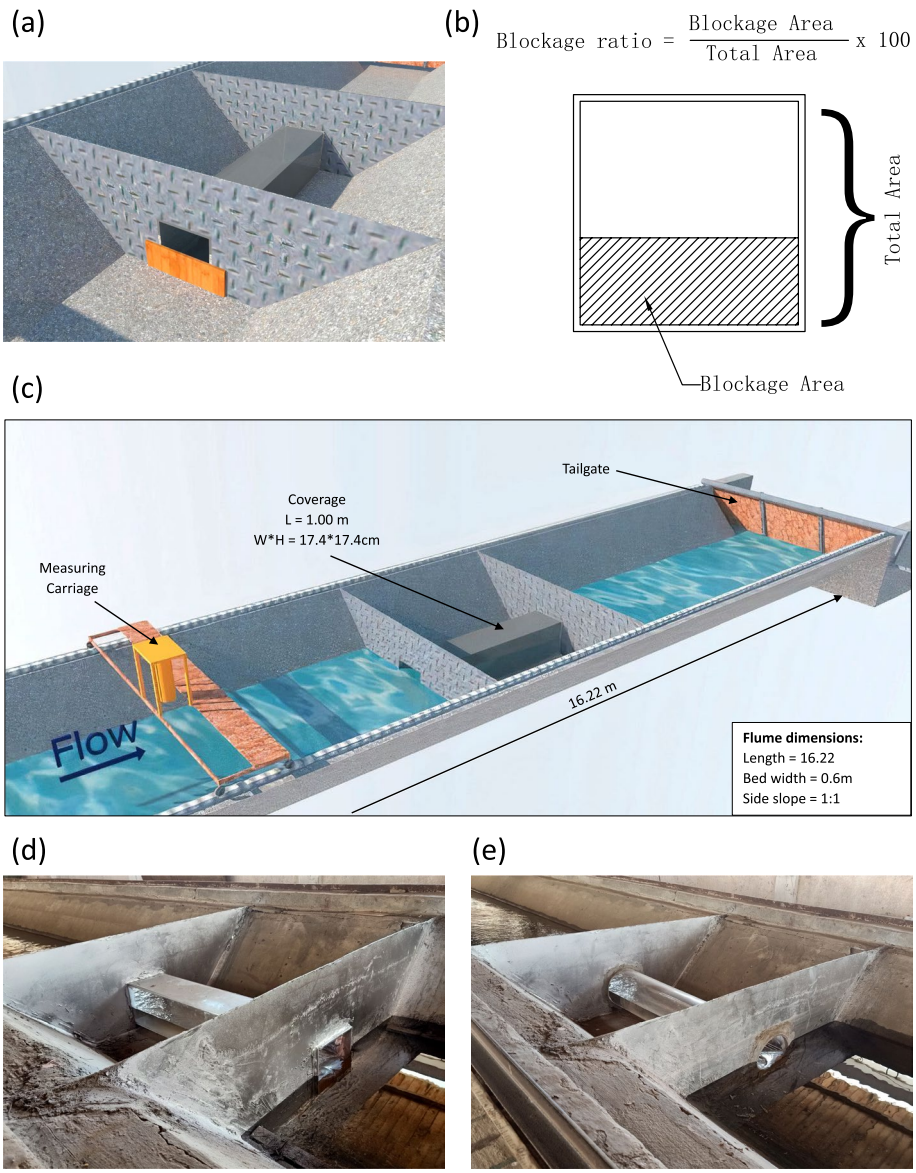

Fig. 4 **a** An isometric view of the blockage within the physical model. **b** The computational method for determining blockage ratios. **c** Isometric depiction of primary components within the experimental setup. **d** An overview of the box section coverage structure. **e** A representation of the circular pipe coverage structure

by the U.S. Department of Commerce [27] and Hotchkiss et al. [28]. Widely utilized by multiple federal agencies, state and local governments, and private industry worldwide [29], HEC-RAS offers an intuitive graphical user interface, extensive options for culvert shapes [30], and robust blockage simulation capabilities [31]. For the open channel flow considered in this study, one-dimensional modelling proved to be sufficient, reinforcing HEC-RAS 1D as the optimal model for this investigation [32, 33].

The HEC-RAS 1D model, developed by the Hydrologic Engineering Centre of the U.S. Army Corps of Engineers (USACE), is engineered to carry out a variety of hydraulic calculations for a network of natural and artificial channels [34]. Recognized for its applicability in hydraulic studies, HEC-RAS was confirmed as the most suitable model for this study. This model was verified through comparisons with results from the experimental work, with particular focus on the pipe and box cross-sectional shapes.

Using the numerical model, 700 runs were performed, encompassing 7 different cross-sectional shapes (square box, pipe, pipe arch, ellipse, arch, conspan arch, and rectangular box), 10 different discharge rates (corresponding to different Froude numbers), and 10 varying blockage ratios. For consistency and accurate comparison, a constant area was maintained for all the studied coverage structures. The blockage ratios were calculated as the percentage of the inlet blockage area relative to the total area of the coverage structure (Fig. 4b).

The final stage of the used methodology involved the evaluation of the results from various hydraulic perspectives, such as water surface profile, heading up, water velocity, water depth ratios, and performance comparisons among the different shapes. The analysis ends up in identifying the best-performing shape under different conditions, providing valuable insights that can enhance the canal design and management strategies.

The experimental work

This study utilized an experimental model to study the effect of inlet blockage in box and pipe canal coverage structures on their hydraulic performance. In addition, the experimental observations were used to verify the numerical model HEC-RAS 1D. The experiment was conducted in a concrete fixed bed trapezoidal flume of 16.22 m length, 0.60 m bed width, 0.42 m depth, and a 1:1 side slope (Fig. 4c). The flume was operated using a recirculating water supply system. A tailgate positioned at the end of the flume allowed the regulation of the water depth.

Two distinct shapes of coverage structures, both 1 m in length, were employed during the experimentation. A box section coverage structure with cross-section dimensions of 17.4×17.4 cm (Fig. 4d) was tested alongside a pipe coverage structure that featured a circular cross-section with a diameter of 20 cm (Fig. 4e). These dimensions were carefully chosen to ensure that the cross-sectional area was approximately constant for both coverage structures. Transparent acrylic fibre was used for the construction of the coverage structures, which were subsequently installed in the concrete flume using steel plates welded at each end to ensure a watertight seal.

A Vectrino 3D velocity sensor and a high-precision point gauge (0.01 cm) were utilized to measure the velocities and water surface profiles, respectively [35]. These instruments were installed on a mobile carriage mounted over the flume. An electronic flow meter was used to measure the inflow discharge, which was installed on the inlet pipe.

The coverage structures were installed in the middle of the flume and tested under four different discharges equating to Froude numbers of 0.047, 0.071, 0.102, and 0.126. To maintain a constant depth upstream of the coverage structure, the tailgate opening was adjusted for each shape. To assess the impact of blockage, blockage ratios of 30%, 50%, and 75% were applied in front of the coverage structure for each discharge. An additional base case of no blockage was also included. The blockage ratios selected for this study encompass a broad spectrum of potential obstruction scenarios, ranging from mild to severe. This selection is grounded in the range of blockage conditions as identified by Rigby et al. [16].

For the experimental study, a total of 32 experimental runs were performed, including 16 runs for each shape (Table 1). Each run consisted of two types of key measurements over a control length of 9 m: the water surface profile and the velocity distribution profile, both measured at the flume's centreline. These measurements were taken in 10 cm increments along the water surface profile and at 20 cm upstream and downstream of the coverage structures for the velocity distribution profiles.

To ensure consistency, each experimental run adhered to a set of procedures: first, installation of the coverage structure; second, flume filling using the underground reservoir; third, valve adjustment for the required discharge; fourth, tailgate adjustment for the desired upstream depth at zero blockage; fifth, calculation and simulation of the blockage depth; and finally, recording of the water depths, surface profiles, and velocity distributions. Following the completion of each run, the parameters were readjusted in preparation for the subsequent run.

The numerical model

For this study, the steady flow water surface profile computation component was used to model diverse canal coverage structure scenarios and their respective blockage ratios. The model computes the water surface profiles from one cross-section to another by solving the energy equation via an iterative procedure, the standard step method [36]. Head loss between any two cross sections includes friction losses and contraction or expansion losses. The friction loss for a canal reach is determined by multiplying the representative friction slope of the reach (S_f) and its discharge weighted length (L).

The data required for modelling were divided into two main categories: geometric data and flow data. Geometric data encompassed the cross-section data, reach lengths, energy loss coefficients, stream junction information, and data related to hydraulic structures (bridges, culverts, spillways, weirs, etc.). In this study, culverts were utilized to simulate canal coverage structures, while gates simulated the tailgate of the flume.

Table 1 A comprehensive overview of the various scenarios and corresponding numbers of simulation runs conducted during the experimental study

Shape of canal coverage structure	Discharges (Q) (l/s)	Froude numbers (Fr)	Blockage ratios (B)	Number of runs per coverage shape	Total
Box	3.0, 4.5, 6.5, and 8.0	0.047, 0.071, 0.102, and 0.126	0%, 30%, 50%, and 75%	$4 \times 4 = 16$	32 runs
Pipe				$4 \times 4 = 16$	

Steady flow data was required for performing steady water surface profile calculations. This included the flow regime (subcritical, supercritical, or mixed), boundary conditions, and discharge information. Boundary conditions establish the initial water surface at the ends of the river system (upstream and downstream). In a subcritical flow regime, the boundary conditions are entered only at the downstream end. The required discharge information is the flow passing through the cross sections of the system, which can be altered at any cross-section within the reach. However, the flow rate cannot be modified within a bridge, culvert, or stream junction.

Verification of the numerical model

To verify the numerical model, it was deployed to investigate the same runs performed using the experimental model (as detailed in Table 1). An identical flume to that used in the experimental model was simulated using HEC-RAS. Each scenario was calibrated by adjusting the tailgate opening to correspond with the water level documented in the experimental model. The Manning coefficient, applied to both the flume and the canal coverage structure, was held constant across all the runs, set at 0.018 and 0.01 respectively. The blockage ratio (B) was converted into a blockage elevation dependent on the canal coverage structure's area, and this value was then utilized as an input in HEC-RAS's blocked obstruction table.

To provide a comparative analysis, the water surfaces produced from the numerical model were compared with the measurements derived from the experimental model for each scenario. Each scenario's measurements were limited to a control length of 9 m, including 3 m upstream, 1 m coverage, and 5 m downstream of the coverage structure. A comparative evaluation of the experimental and numerical water depth outcomes for the box coverage structure is exhibited in Fig. 5, while Fig. 6 presents a similar comparison for the pipe coverage structure. To calculate the root mean square error (RMSE) and the relative error (E), each experimental measurement point was compared with its corresponding result from the numerical model. This process was repeated across all measurement locations for the 32 runs, yielding a total of 1312 measurements. The calculated average relative error was 3.8%, with a standard deviation of 1.2%. Potential contributing factors to this deviation may include human error during measurements or fluctuations in the water surface. These findings emphasize the precision and reliability of the HEC-RAS 1D numerical model for simulating the studied research problem.

The numerical model's output velocity represents the average cross-section velocity. However, in the experimental work, velocity was measured at several cross-section depths using the Vectrino 3D velocity sensor, with measurements taken at 1 cm intervals. The experimentally measured average velocity was estimated by averaging the velocities recorded at 0.2 of the water depth and 0.8 of the water depth. The comparison of the numerically modelled velocities and the experimentally measured velocities is depicted in Fig. 7. Here, the red dashed line symbolizes the ideal case where modelled and measured velocities coincide, with values closer to this line representing superior model performance. The coefficient of determination (R^2) was calculated

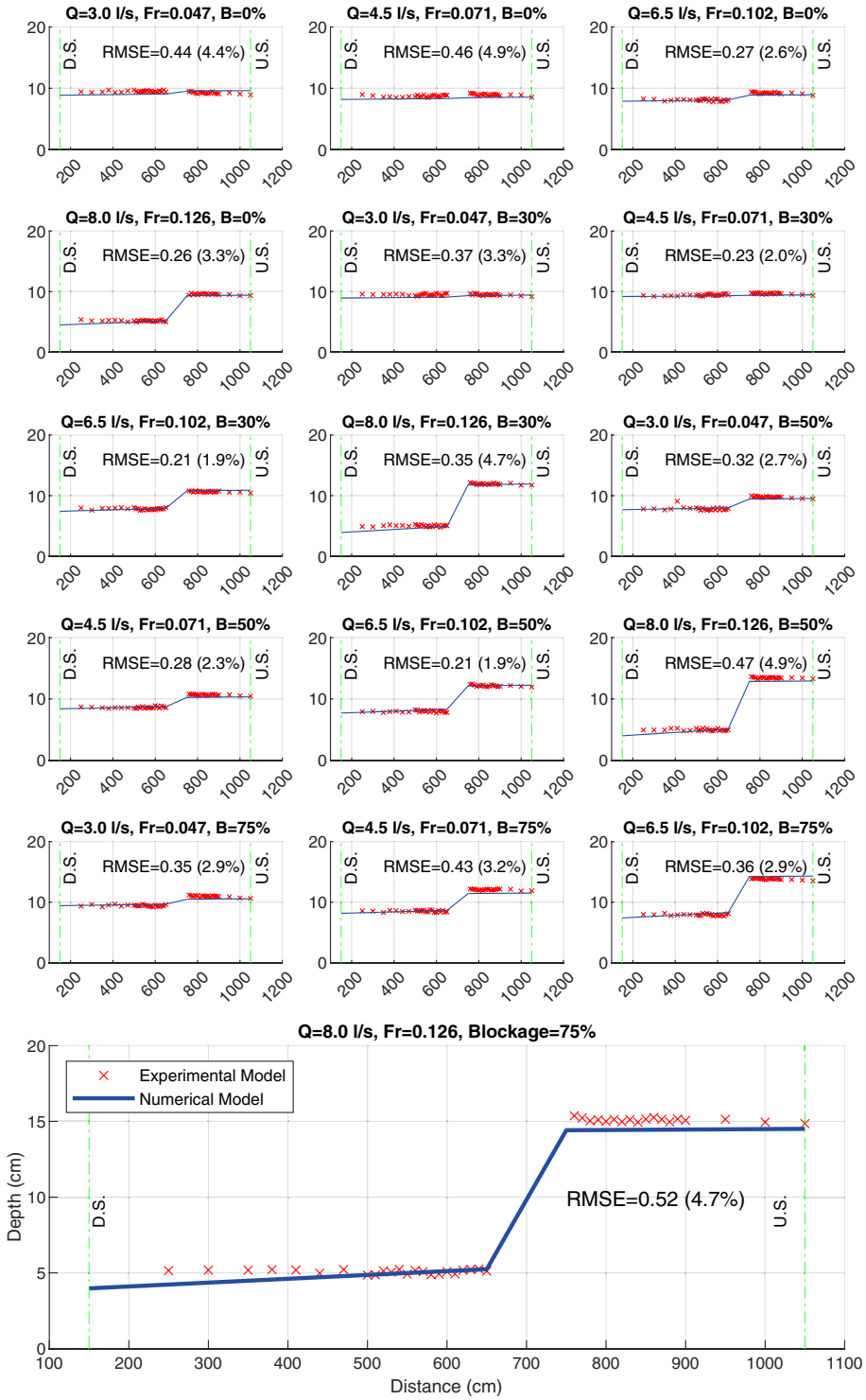

Fig. 5 Verification results for the water depth across 16 runs of the box coverage structure, with a control length of 9 m

for each blockage ratio for the velocities both upstream and downstream of the coverage structure. The R^2 average across all results is 0.76, with a standard deviation of 0.15. This R^2 value is deemed acceptable (above 0.7) for all scenarios, apart from the

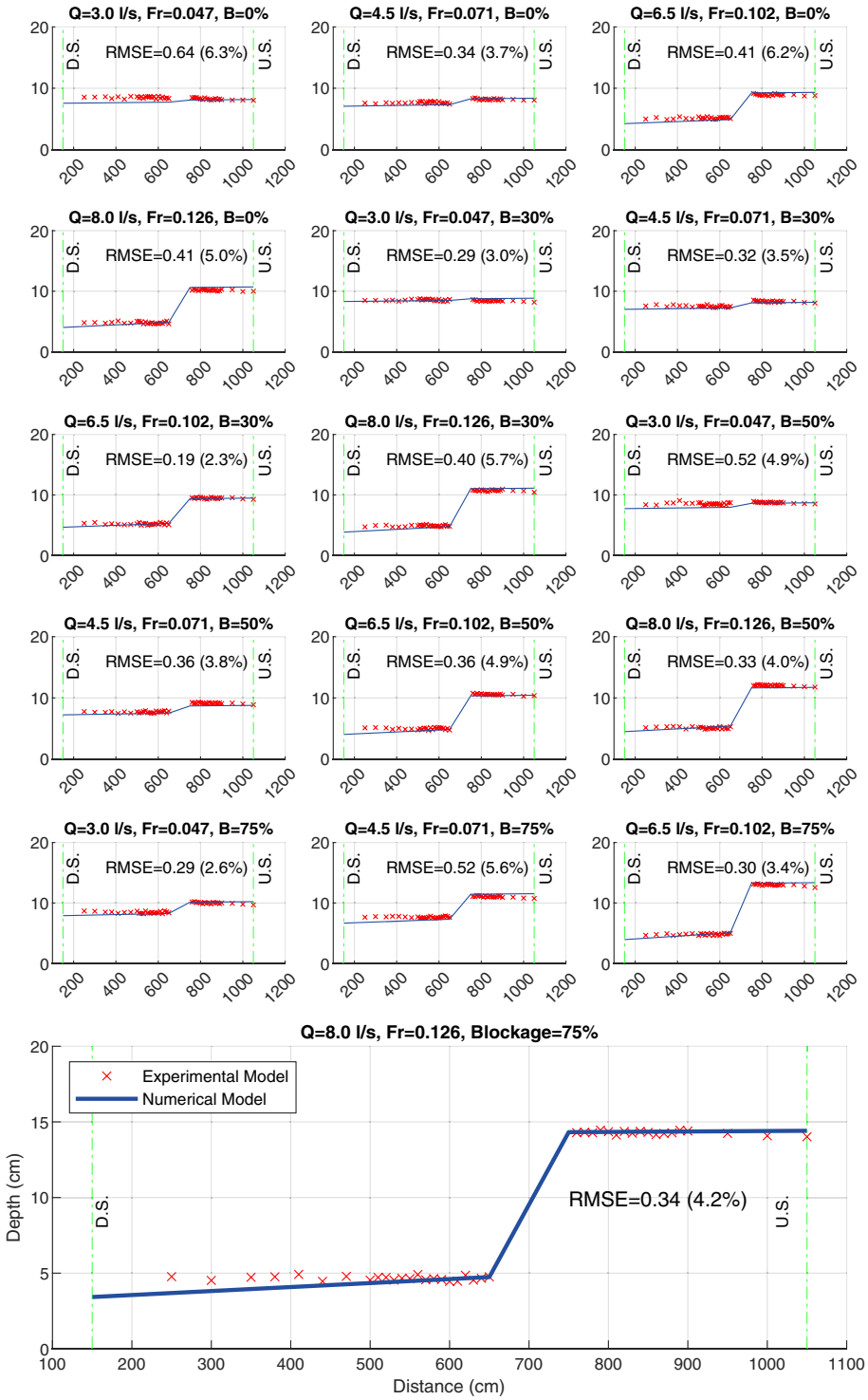

Fig. 6 Verification results for the water depth across 16 runs of the pipe coverage structure, with a control length of 9 m

upstream velocity in the scenario with the highest blockage ratio (75%). This discrepancy may be due to extremely low velocities, which could distort the measurements of horizontal velocity and amplify their uncertainty.

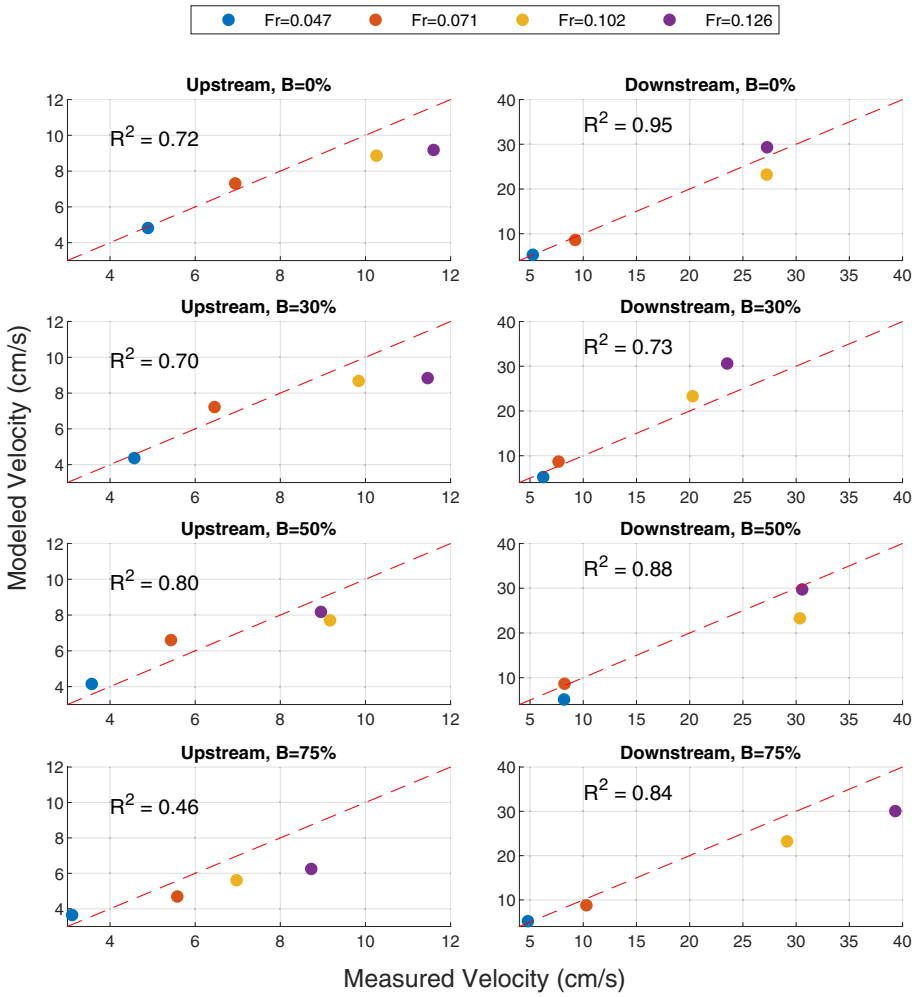

Fig. 7 Verification results illustrating velocity variations upstream and downstream of the coverage structure for different blockage ratios

Study area

Following the verification of the numerical model, the 1–1 branch canal at Northern Sinai was chosen as a real-life case to examine the implications of altering the coverage structure's shape with varying blockage ratios (Fig. 8). This branch canal is a part of the Central Administration of Water Resources and Irrigation's network in North Sinai. The canal spans a total length of 5.03 km, with a base width of 1.50 m, side slopes of 2:1 (H:V), and a longitudinal slope of 12 cm/km. The selected section for this study is a 2.1-km stretch commencing from the canal's intake, with the canal's design information sourced from the National Water Research Center–Channel Maintenance Research Institute [37] and detailed in Table 2.

A canal coverage structure of 100 m length and a cross-sectional area of 1.54 m^2 was investigated under varying shapes and blockage ratios. For the entire modelled section, interpolated cross-sections were added at every 100 m, while for the 100 m segments preceding and following the coverage, interpolations were made every 10 m to represent the water surface more accurately at these locations. Given that this reach is downstream

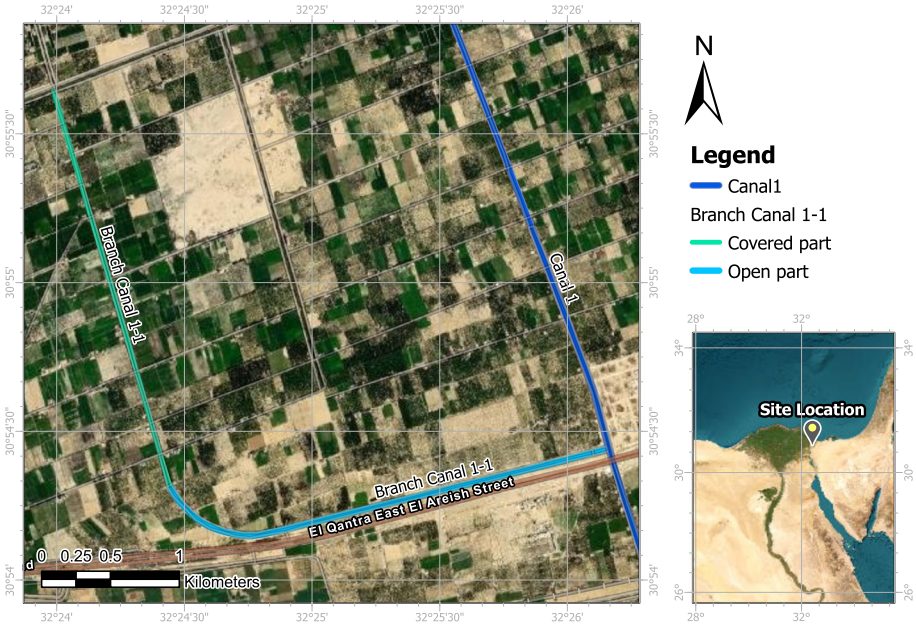

Fig. 8 A map demonstrating the specific location and configuration of the investigated canal, Branch Canal 1–1

Table 2 The design data of Branch Canal 1–1 [37]

Location	Bed levels (m)	Water levels (m)	Berm levels (m)	Bank levels (m)	Bed width (m)	Bed slope (cm/km)	Side slopes	Discharge (m^3/s)
Intake of the canal	6.99	7.82	8.58	9.58	1.5	12	2:1	0.72
2.1 km from the intake	6.73	7.56	8.32	9.32				

controlled, the downstream boundary condition of the modelled section was set as the normal depth with a bed slope of 12 cm/km. For the Branch canal 1–1 case study, the model calibration relied on the canal's design data and the two measured water surface elevations at the upstream and downstream extremities of the studied reach. Manning's roughness coefficient of 0.025 was utilized to achieve the precise water surface elevations, measured as 7.82 m upstream (at station 2.10 km) and 7.56 m downstream (at station 0.00 km).

In the study, seven different shapes of canal coverage structures were modelled: pipe, square box, pipe arch, ellipse, arch, conspan arch, and rectangular box (as depicted in Fig. 9). All shapes were designed to have dimensions that result in an equivalent area of 1.54 m^2, as shown in Table 3. Ten different canal discharges, corresponding to 10 Froude numbers and ranging between the maximum design discharge of 0.72 m^3/s and a minimum discharge of 0.1 m^3/s, were modelled. Additionally, 10 different blockage ratios, ranging from 0 to 90%, were simulated for each case. Entrance and exit loss coefficients of the canal coverage structures were set at 0.5 and 1 respectively, with Manning's

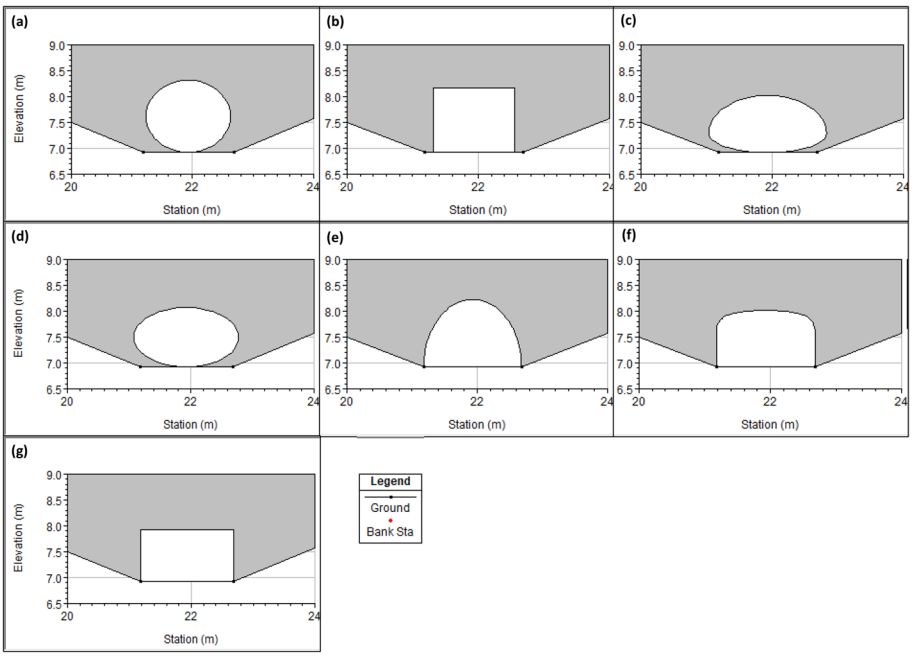

Fig. 9 The different shapes of the canal coverage structure shapes simulated within the HEC-RAS model: **a** pipe, **b** square box, **c** pipe arch, **d** ellipse, **e** arch, **f** conspan arch, and **g** rectangular box

Table 3 Summary table on the shapes and dimensions of the canal coverage structures under investigation

Shape of canal coverage structure	Height (m)	Width (m)
Pipe	1.40	1.40
Square box	1.24	1.24
Pipe arch	1.10	1.80
Ellipse	1.15	1.70
Arch	1.31	1.50
Conspan arch	1.10	1.50
Rectangular box	1.03	1.50

Table 4 A tabulated summary of the different modelling scenarios employed in the numerical model for the case study of Branch Canal 1–1

Shape of canal coverage structure	Discharge (Q) (m^3/s)	Froude number (Fr)	Blockage ratio (B) (%)	Number of scenarios
Pipe Square box Pipe arch Ellipse Arch Conspan arch Rectangle box	0.72, 0.65, 0.58, 0.51, 0.44, 0.38, 0.31, 0.24, 0.17, and 0.10	0.1211, 0.1204, 0.1196, 0.1187, 0.1177, 0.1167, 0.1153, 0.1136, 0.1112, and 0.1076	0, 10, 20, 30, 40, 50, 60, 70, 80, and 90%	7 coverage shapes ×10 discharge values ×10 blockage ratios = 700 scenarios

roughness coefficient maintained at a constant value of 0.018. A total of 700 scenarios were examined to cover these cases, which are summarized in Table 4.

Results

Results of the experimental model

This subsection focuses on the results derived from the experimental model, with a special emphasis on the box and pipe sections as the most common shapes of the canal coverage structure. The primary performance metric used in this study is the dh/ho ratio, where 'dh' represents the differential in water level upstream and downstream the coverage structure, and 'ho' corresponds to the baseline water level upstream of the coverage structure. Lower values of this ratio signify a more efficient water flow and thus indicate an enhanced performance of the coverage structure.

Figure 10 features a box plot encapsulating the dh/ho values for both the box and pipe sections, as observed in the experimental model. Each plot visually depicts the dh/ho values from 16 scenarios pertinent to each section, as detailed in Table 1.

The average dh/ho value was computed to be 0.35 for the pipe section, hinting at marginally superior efficiency compared to the box section, which recorded a mean dh/ho value of 0.39. These results give valuable insights into the comparative performance of the two canal coverage structures under a variety of conditions. It is apparent from these findings that the pipe section demonstrated superior performance to the box section in terms of water flow efficiency.

Effect of the blockage ratio on the performance of canal coverage structure

For an assessment of results in a dimensionless format, the quantity dh/ho was calculated for each scenario, where dh refers to the difference in upstream and downstream water levels across the coverage structure (reflecting the head loss) and ho is the normal canal depth prior to the addition of a coverage structure. The velocity ratio, V/Vo, presents another useful metric for assessing canal coverage structure performance; V represents the velocity upstream of the coverage structure, while Vo represents the velocity at the same point in the absence of blockage.

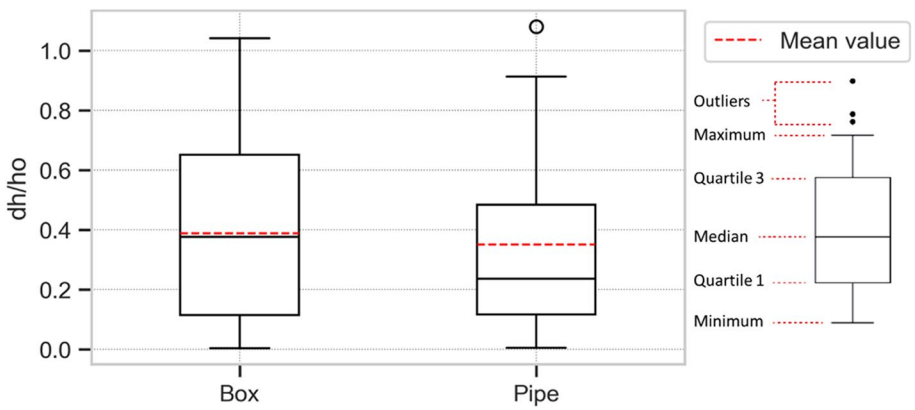

Fig. 10 Box plot of dh/ho values for the pipe and box coverage sections from the experimental model (left), alongside a sample box plot illustrating the different components of a typical box plot (right)

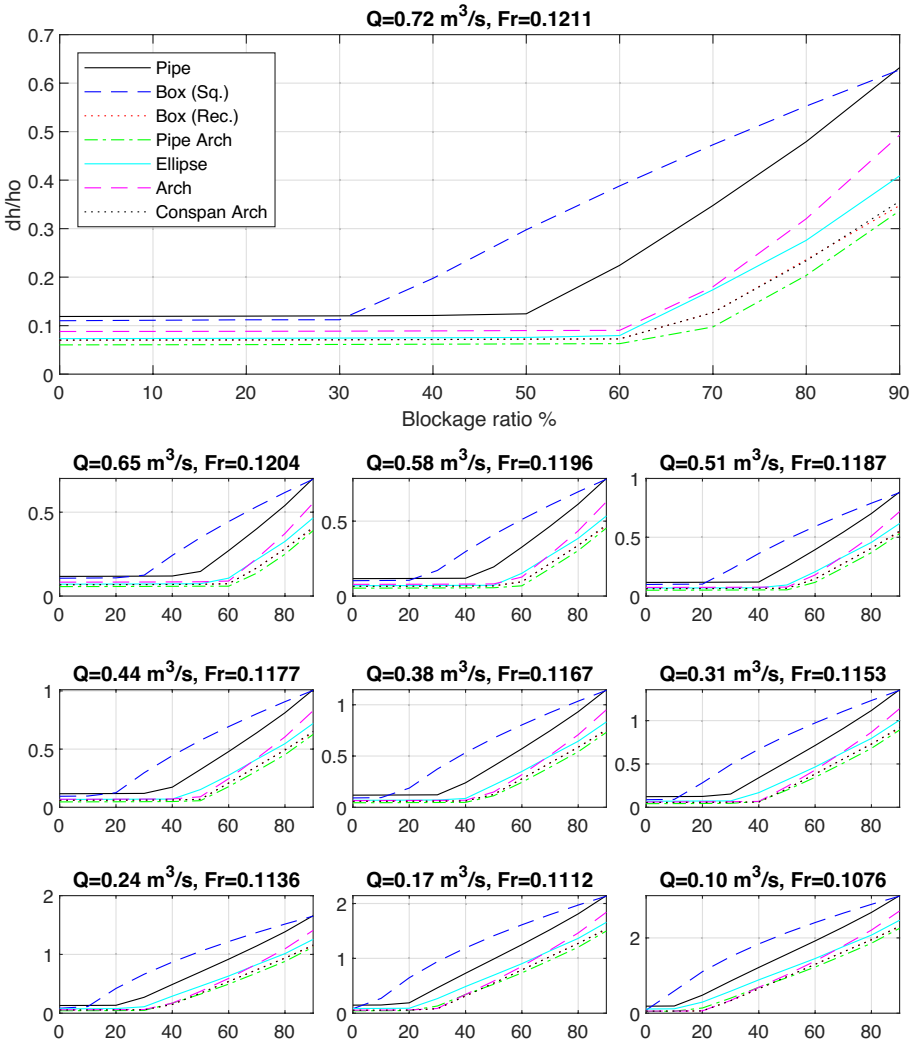

Fig. 11 A graphical representation of dh/ho results for different blockage ratios and coverage shapes

Figure 11 presents the results for dh/ho across the different modelled scenarios and coverage shapes. Lower dh/ho values are preferred, as these indicate a minimal head loss. As can be seen from the figure, the performance of the coverage structure degrades with increased blockage, leading to an amplified head loss. The detrimental impact of blockage is more pronounced with higher blockage ratios, thereby reducing the efficiency of the coverage structure. The results also highlight the square box as the most susceptible to blockage effects, demonstrating the worst performance among all coverage shapes, followed by the pipe coverage. At the design flow of 0.72 m^3/s (Fr = 0.1211), the square box section begins to exhibit the effects of blockage at a blockage ratio of 30%, while the pipe coverage is affected at a 50% blockage ratio. The remaining coverage structures demonstrate a resistance to blockage effects until a blockage ratio of 60% is reached. Across all scenarios, the square box consistently shows the worst performance, with blockage effects beginning to manifest at a blockage ratio of approximately 10%. The pipe arch structure, on the other hand,

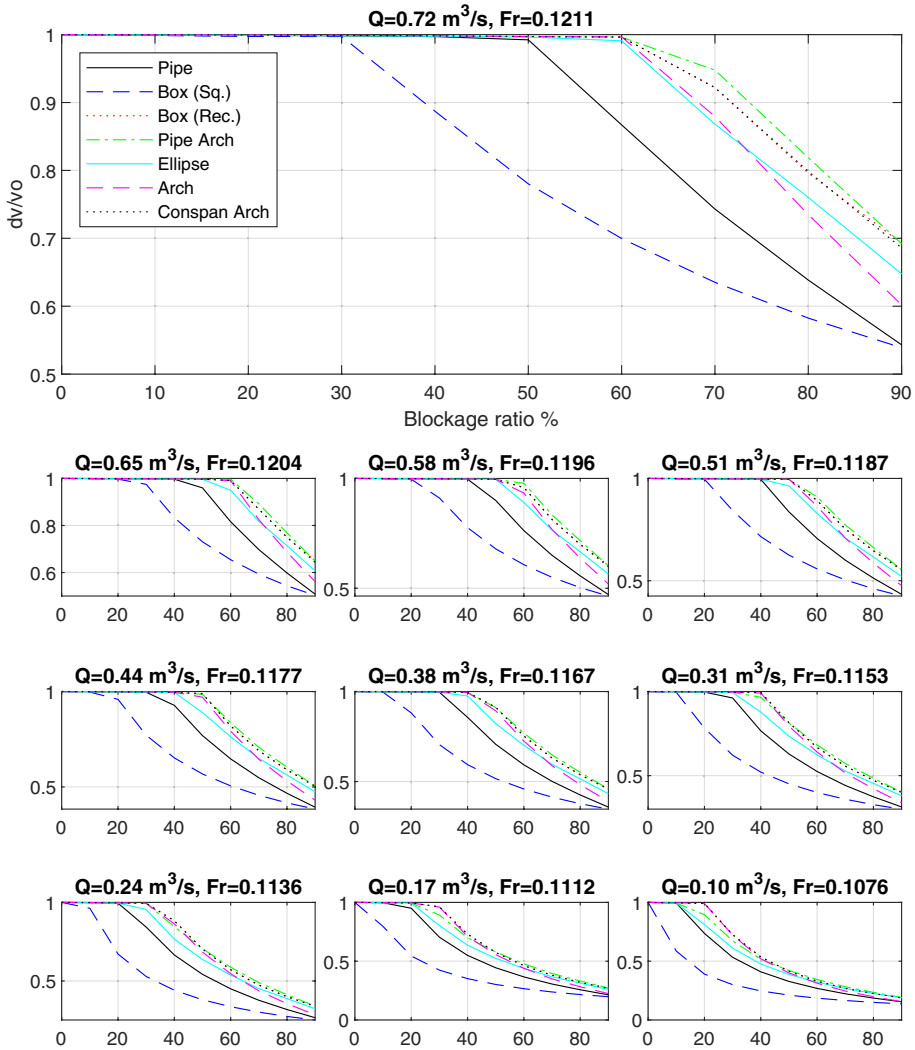

Fig. 12 A graphical representation of V/Vo results for different blockage ratios and coverage shapes

exhibits the most robust performance across all scenarios, followed closely by the rectangular box and conspan arch, both of which demonstrate similar performance characteristics.

Figure 12 displays the V/Vo results for the modelled scenarios and coverage shapes. Higher V/Vo values are preferred as they correspond to minimal velocity reduction and thus a decreased sedimentation rate. The effect of blockage on velocity reduction is particularly evident at lower Froude numbers, and an increase in the blockage ratio leads to further reductions in velocity for all coverage structure shapes studied. These findings underscore the detrimental impact of blockage on the performance of coverage structures. Again, the square box appears to be the least effective coverage shape, with pipe coverage following closely as the second least effective. Conversely, the pipe arch demonstrates the most effective performance amongst coverage shapes, closely followed by the rectangular box and conspan arch.

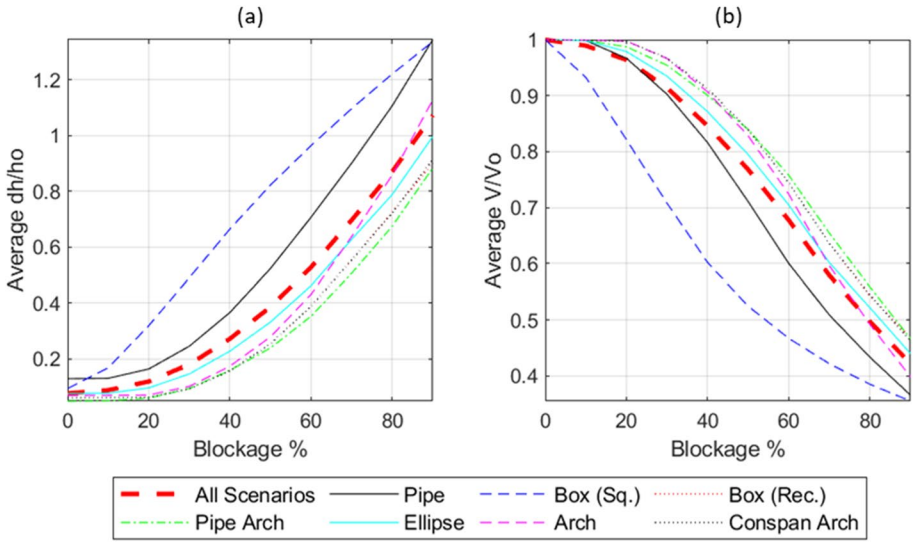

Fig. 13 Graphical results depicting the average of all Froude numbers (the overall average result of all shapes is the red dashed line) **a** Average results of dh/h_o. **b** Average results of V/V_o

To enhance the understanding of the overarching effects of blockage, the mean values of dh/ho and V/Vo across the entire range of Froude numbers were calculated. The graph in Fig. 13a displays the average dh/ho results for all studied Froude numbers. The collective average dh/ho outcome, for every shape, is represented by a red dashed line. In contrast, the individual outcomes for different coverage shapes are indicated by diverse line types and hues. The dh/ho results show an upward inflection in the slope of the dashed line around the 30% blockage ratio mark, signifying a critical maintenance threshold. Beyond a blockage ratio of 30%, coverage structure maintenance becomes necessary to maintain satisfactory performance. With the exception of the square box coverage, which displays performance deterioration at a mere 10% blockage ratio, all shapes appear to mimic the average trend indicated by the red dashed line. Consequently, the square box coverage proves to be the most demanding in terms of maintenance.

Moving to Fig. 13sb, the V/Vo ratio is presented for the average Froude number in a similar fashion. The mean results reveal a precipitous drop around a blockage ratio of 20%. Among all shapes, the pipe arch stands out as the best performer with respect to velocity. All coverage shapes tend to align with the average trend, with the notable exception of the square box shape. It demonstrates a more pronounced reduction in the velocity ratio at earlier stages of blockage, marking it as the least efficient performer overall.

Effect of the shape of the canal coverage structure

In this section, the impact of changing the coverage structure's shape on its performance is assessed through evaluating the head loss ratio (dh/ho) and velocity ratio (V/Vo).

Figure 14 presents a comprehensive view of the average dh/ho and V/Vo across all the studied Froude numbers and blockage ratios. The standout performance of the

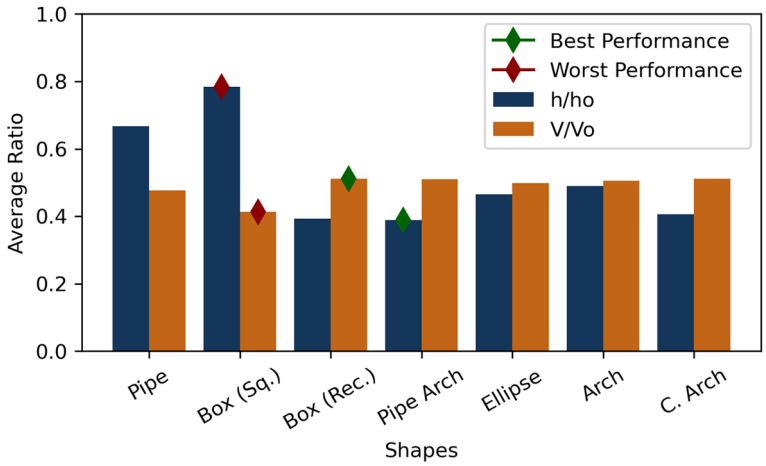

Fig. 14 A summary of average results for dh/ho (lower values are preferable) while for V/Vo (higher values are preferable) for all blockage ratios, with the best performing shapes marked by a green diamond and the least efficient shapes marked by a red diamond

pipe arch coverage shape is underlined in the figure, with the shape marked by a green diamond signifying its superiority in terms of head loss reduction. Interestingly, the square box structure's performance, though inferior, contrasts with the superior performance of the rectangular box structure. The latter, with a height to width ratio of 2:3, emerges as the second-best performer.

On the same plot, the average V/Vo indicates the rectangular box structure's (H:W = 2:3) exceptional ability to maintain upstream velocity. Both the rectangular box and the pipe arch coverage demonstrate similar V/Vo values across all blockage ratios, suggesting comparable performance characteristics. Therefore, the choice between these two shapes could be influenced by factors other than hydrodynamic considerations, such as construction complexity or cost considerations.

Discussion

The research objectives of this study were primarily focused on a thorough analysis of the impacts of blockage at the inlet of canal coverage structures of various shapes on their key hydraulic parameters, especially the water levels and velocities. Experimental and numerical modelling methodologies were utilized to enable this comprehensive evaluation, with the primary aim of establishing the optimal design and management practices for canal coverage structures.

A noteworthy achievement in the study was the successful verification of the numerical model. The model exhibited a high degree of accuracy, as reflected by the average relative error of 3.8% and a standard deviation of 1.2%. This data validates the reliability of the numerical model and affirms its efficacy in simulating complex hydraulic scenarios, a requirement that is fundamental to the intricate objectives of the research.

Subsequent analysis investigating the impact of blockage ratio on canal coverage structures' performance unveiled several significant insights. As the blockage ratio increased, a consequential rise in the head loss (dh/ho) and a decrease in the velocity ratio (V/Vo) occurred, indicating a negative effect on the structures' performance.

In the present study, different canal coverage structure shapes were found to have varying degrees of vulnerability to blockage. The square box and pipe structures were particularly susceptible, while the pipe arch, rectangular box, and conspan arch structures demonstrated greater resilience under increased blockage conditions. These findings offer valuable, evidence-based guidance on the implications of blockage ratios for canal coverage structures' design and management.

The evaluation of different canal coverage structures and their impact on the hydraulic performance produced enlightening results. The pipe arch structure excelled in minimizing head loss, while the rectangular box shape (H:W = 2:3) maintained upstream velocity most effectively. These findings contrast with those of Miranzadeh et al. [25], who recommended box culverts over circular pipe culverts due to the latter's higher blockage levels.

Despite the enlightening findings, the present study does have limitations. The HEC-RAS 1D numerical model used in the study might not completely represent the complexity of fluid dynamics in 3D environments. Moreover, the blockage method selected for the study may not cover all the possible scenarios. Finally, the experimental model was based on a scaled-down canal system, and its findings may not directly apply to full-scale, real-world situations.

In conclusion, the study contributes to the understanding of blockage and structure shape implications on canal coverage structures' hydraulic performance. In addition, it offers data-driven insights to practitioners in the field, facilitating informed decisions in canal coverage structure design and management for optimal hydraulic performance.

Conclusions

This research aimed at evaluating the impact of blockage on hydraulic parameters of variously shaped canal coverage structures. Several key insights have yielded through the comprehensive application of experimental and numerical modelling techniques.

- Impact of blockage ratio: The results highlight the negative correlation between the blockage ratio and the performance of canal coverage structures. An increase in blockage ratio led to an amplification in the head loss ratio and a decrease in the velocity ratio. This underlines the need for proactive monitoring and maintenance of these structures to prevent blockage and ensure their optimal performance.
- Influence of coverage structure's shape: The shape of the canal coverage structure significantly impacts its resilience to blockage and overall performance. Among the shapes examined, the pipe arch showed the least increase in head loss, while the rectangular box structure (H:W = 2:3) demonstrated minimal reduction in upstream velocity. Conversely, the square box and pipe structures exhibited greater vulnerability to increased blockage.

From these findings, it can be inferred that the choice of shape in the design of canal coverage structures can greatly influence their efficiency and blockage resilience. While the pipe arch structure emerged as the best performer in terms of head loss reduction, the rectangular box structure (H:W = 2:3) showcased superior maintenance of upstream

velocity. Therefore, these should be the preferred choices considering their robust performance under increasing blockage.

To summarize, this research provides a significant contribution towards a more profound understanding of the effects of blockage and structural shape on the performance of canal coverage structures. Future studies are suggested to expand on this research by exploring additional factors impacting the performance of canal coverage structures, such as material composition, or by testing these findings in diverse hydraulic contexts. Another potential avenue for further research could be a cost–benefit analysis integrating these findings, promoting more economically viable and efficient canal coverage structure designs.

Abbreviations

1D	One dimensional
B	Blockage ratio
BOD	Biological oxygen demand
dh	Difference in water level upstream and downstream the coverage structure
DO	Dissolved oxygen
E	Relative error
Fr	Froude number
HEC-RAS	Hydrologic Engineering Center-River Analysis System
ho	Baseline water level upstream the canal coverage structure
H :V	Horizontal to vertical ratio (width to height ratio)
L	Discharge weighted length
Q	Discharge
Sf	Friction slope of the reach [dimensionless]
R^2	Coefficient of determination
RMSE	Root mean square error
V	The velocity upstream of the canal coverage structure
Vo	The velocity at the same point in the absence of blockage
USACE	United States Army Corps of Engineers

Acknowledgements
Not applicable.

Authors' contributions
DAA: collecting the literature, performing the experimental work, running the numerical model, analyzing and interpreting the results, and writing the paper as a part of her M.Sc. thesis at the irrigation and hydraulics Department, Faculty of Engineering, Ain Shams University. NMA: analyzing and interpreting the results, and supervising and revising the paper as the main supervisor of the first author's M.Sc. thesis. DAE: analyzing and interpreting the results, writing the paper, and supervising and revising the paper as the second supervisor of the first author's M.Sc. thesis. All the authors read and approved the final paper.

Authors' information
Eng. Doaa Ahmed Abo-Sreeaaa (DAA), currently works at the National Water Research Centre. She Received the B.Sc. degree in 2014 from the Irrigation and Hydraulics Department, Faculty of Engineering, Cairo University, Cairo, Egypt. She is currently studying M.Sc. degree at the Irrigation and Hydraulics Department, Faculty of Engineering, Ain Shams University.
Prof. Dr. Nahla Mohamed AboulAtta (NMA), currently works as a Professor of Irrigation Design at the Irrigation and Hydraulics Department, Faculty of Engineering, Ain Shams University, Cairo, Egypt. B.Sc. and M.Sc. from Ain Shams University, Ph.D. was a joint venture between Ain Shams University, Egypt and Penn State University, United States.
Dr. Doaa Anas El-Molla (DAE), currently works as an Associate Professor, Irrigation & Hydraulics Department, Faculty of Engineering, Ain Shams University, Cairo, Egypt. She received the Ph.D. degree in 2014, M.Sc. degree in 2009, and B.Sc. degree in 2004, all from, Irrigation and Hydraulics Department, Faculty of Engineering, Ain Shams University.

Funding
This study had no funding from any resource.

Availability of data and materials
All data generated or analysed during this study are included in this published article.

Declarations

Competing interests
The authors declare that they have no competing interests.

Received: 3 May 2023 Accepted: 22 June 2023
Published online: 07 July 2023

References

1. Velasco-Muñoz JF, Aznar-Sánchez JA, Batlles-delaFuente A, Fidelibus MD (2019) Sustainable irrigation in agriculture: an analysis of global research. Water
2. Yarnell DL, Nagler FA, Woodward SM (1926) Flow of water through culverts. The University
3. B.E. van den Bosch, J. Hoevenaars, C. Brouwer (1992) Irrigation water management training manual CANALS. FAO Land and Water Development Division
4. Olmsted TR, Dukes MD (2011) Frequency of residential irrigation maintenance problems: AE472/AE472, 1/2011. EDIS 2011:. https://doi.org/10.32473/edis-ae472-2011
5. El-Molla DA, El-Molla MA (2021) Seepage losses from trapezoidal earth canals with an impervious layer under the bed. Water Practice and Technology 16:530–540. https://doi.org/10.2166/wpt.2021.010
6. Hrozencik RA, Potter NA, Wallander S (2022) The cost effectiveness of irrigation canal lining and piping in the Western United States. In: American Agriculture, Water Resources, and Climate Change. University of Chicago Press, Chicago, USA.
7. Samir A, El Shiekh H, El-Dawy M, El-Zayat Y, El-Molla D (2023) Water losses from irrigation canals and their modern sustainable solutions -a review, In Proceedings of the International Conference on Smart Cities, 861–886. Cairo, Egypt, March 2023.
8. Abd-Elaty I, Pugliese L, Bali KM, Grismer M, Eltarabily M (2022) Modelling the impact of lining and covering irrigation canals on underlying groundwater stores in the Nile Delta, Egypt. Hydrological Processes 36:. https://doi.org/10.1002/hyp.14466
9. McKuin B, Zumkehr A, Ta J et al (2021) Energy and water co-benefits from covering canals with solar panels. Nat Sustain 4:609–617. https://doi.org/10.1038/s41893-021-00693-8
10. Pawar P, Pondkule A, Waychal P, et al (2019) The remedial measures for reduction of losses in existing canal system.
11. El Baradei S, Alsadeq M (2018) Impact of covering irrigation canals on evaporation rates in arid areas. In: Proceedings of International Structural Engineering and Construction
12. MWRI (2016) https://www.facebook.com/mwrifb. Accessed 1 Apr 2021
13. Iqbal U, Barthelemy J, Perez P (2022) Prediction of hydraulic blockage at culverts from a single image using deep learning. Neural Comput & Applic 34:21101–21117. https://doi.org/10.1007/s00521-022-07593-8
14. Meegoda JN, Zou Z (2015) Long-term maintenance of culvert networks. Journal of Pipeline Systems Engineering and Practice 6:04015003. https://doi.org/10.1061/(ASCE)PS.1949-1204.0000194
15. Agbola BS, Ajayi O, Taiwo OJ, Wahab BW (2012) The August 2011 flood in Ibadan, Nigeria: Anthropogenic causes and consequences. Int J Disaster Risk Sci 3:207–217. https://doi.org/10.1007/s13753-012-0021-3
16. Rigby EH, Boyd MJ, Roso S, et al (2002) Causes and effects of culvert blockage during large storms. In: Ninth International Conference on Urban Drainage (9ICUD). Doubletree Hotel, Portland, Oregon, United States, pp 1–16
17. Mulahasan S, Al-Mohammed FM, Al-Madhhachi AST (2021) Effect of blockage ratio on flow characteristics in obstructed open channels. Innovative Infrastructure Solutions. https://doi.org/10.1007/s41062-021-00592-z
18. Kramer M, Peirson WL, French R, Smith GP (2015) A physical model study of culvert blockage by large urban debris. Australasian Journal of Water Resources 19:127–133. https://doi.org/10.1080/13241583.2015.1116184
19. Barthelmess AJ, Rigby EH (2011) Estimating coverage and bridge blockages-a simplified procedure. In: Proceedings of the 34th World Congress of the International Association for Hydro-Environment Research and Engineering: 33rd Hydrology and Water Resources Symposium and 10th Conference on Hydraulics in Water Engineering. Australia, p 39
20. Sorourian S, Keshavarzi A, Samali B, Ball J (2014) Prediction of scouring depth at the outlet of partially blocked box culvert. In: World Environmental and Water Resources Congress 2014: Water Without Borders - Proceedings of the 2014 World Environmental and Water Resources Congress. Portland, Oregon
21. Sorourian S (2015) Turbulent flow characteristics at the outlet of partially blocked box culverts. In: 36th IAHR World Congress. Netherlands
22. Shahat ZT, Ellean AS, Sief HM, Sobeih MF (2018) Assessment the impact of covering a part of watercourse by pipe. Australian J Basic Appl Sciences 12:113–120. https://doi.org/10.22587/ajbas.2018.12.12.19
23. Karimpour S, Gohari S (2020) An experimental study on the effects of debris accumulation at the culvert inlet on downstream scour. J Rehab Civil Eng 8:184–199. https://doi.org/10.22075/jrce.2020.18210.1348
24. Osman EA, Taha Z (2022) Impact of box section coverage on the hydraulic parameters of open channels. Water Practice and Technology. https://doi.org/10.2166/wpt.2021.103
25. Miranzadeh A, Keshavarzi A, Hamidifar H (2022) Blockage of box-shaped and circular culverts under flood event conditions: a laboratory investigation. Int J River Basin Manag 0:1–10. https://doi.org/10.1080/15715124.2022.2064483
26. Sorourian S, Keshavarzi A, Ball J, Samali B (2014) Blockage effects on scouring downstream of box culverts under unsteady flow. Australasian J Water Resources 18:180–190. https://doi.org/10.1080/13241583.2014.11465449
27. U.S. Department of Commerce (2007) Technical Report, Evaluation of Different Hydraulic Models iIn Support Of National Weather Service Operations, Project Title: Evaluation of Hydraulic Models in Support of NWS Operations
28. Hotchkiss RH, Thiele EA, Nelson EJ, Thompson PL (2008) Culvert hydraulics: comparison of current computer models and recommended improvements. Transp Res Rec 2060:141–149
29. Indiana Department of Natural Resources (2016) GUIDELINES FOR HYDRAULIC MODELING USING HEC-RAS. In: The General Guidelines for the Hydrologic-Hydraulic Assessment of Floodplains in Indiana. p 13
30. Chris Maeder (2020) HEC-RAS culvert types, shapes and dimensions. In: Knowledge Base on CivilGEO. https://knowledge.civilgeo.com/knowledge-base/hec-ras-culvert-types-shapes-dimensions/. Accessed 28 May 2023

31. Lee K, Ho Y-H, Chyan Y-J (2006) Bridge blockage and overbank flow simulations using HEC–RAS in the Keelung River during the 2001 Nari Typhoon. Journal of Hydraulic Engineering-asce - J HYDRAUL ENG-ASCE 132:. https://doi.org/10.1061/(ASCE)0733-9429(2006)132:3(319)
32. Hodges BR (2020) An artificial compressibility method for 1D simulation of open-channel and pressurized-pipe flow. Water 12:1727. https://doi.org/10.3390/w12061727
33. Luo H, Fytanidis DK, Schmidt AR, García MH (2018) Comparative 1D and 3D numerical investigation of open-channel junction flows and energy losses. Adv Water Resour 117:120–139. https://doi.org/10.1016/j.advwatres.2018.05.012
34. HEC-RAS User's Manual (2016). https://www.hec.usace.army.mil/confluence/rasdocs/rasum/latest. Accessed 28 May 2023
35. Vectrino - 3D Water Velocity Sensor Lab Probe | Environmental XPRT (2017). https://www.environmental-expert.com/downloads/vectrino-3d-water-velocity-sensor-lab-probe-datasheet-834473. Accessed 28 May 2023
36. Molinas A, Yang CT (1985) Generalized water surface profile computations. J Hydraul Eng 111:381–397. https://doi.org/10.1061/(ASCE)0733-9429(1985)111:3(381)
37. National Water Research Center – Channel Maintenance Research Institute (2020) Technical Report, Study of Maximizing Coverage Performance on Branch Canal (1–1). Egypt, Cairo